Paired analysis of TCRα and TCRβ chains at the single-cell level in mice

Pradyot Dash,[1] Jennifer L. McClaren,[1] Thomas H. Oguin III,[1] William Rothwell,[1] Brandon Todd,[1] Melissa Y. Morris,[1] Jared Becksfort,[1] Cory Reynolds,[1] Scott A. Brown,[1] Peter C. Doherty,[1,2] and Paul G. Thomas[1]

[1]St Jude Children's Research Hospital, Memphis, Tennessee, USA. [2]Department of Microbiology and Immunology, University of Melbourne, Melbourne, Victoria, Australia.

Characterizing the TCRα and TCRβ chains expressed by T cells responding to a given pathogen or underlying autoimmunity helps in the development of vaccines and immunotherapies, respectively. However, our understanding of complementary TCRα and TCRβ chain utilization is very limited for pathogen- and auto-antigen-induced immunity. To address this problem, we have developed a multiplex nested RT-PCR method for the simultaneous amplification of transcripts encoding the TCRα and TCRβ chains from single cells. This multiplex method circumvented the lack of antibodies specific for variable regions of mouse TCRα chains and the need for prior knowledge of variable region usage in the TCRβ chain, resulting in a comprehensive, unbiased TCR repertoire analysis with paired coexpression of TCRα and TCRβ chains with single-cell resolution. Using CD8+ CTLs specific for an influenza epitope recovered directly from the pneumonic lungs of mice, this technique determined that 25% of such effectors expressed a dominant, nonproductively rearranged Tcra transcript. T cells with these out-of-frame Tcra mRNAs also expressed an alternate, in-frame Tcra, whereas approximately 10% of T cells had 2 productive Tcra transcripts. The proportion of cells with biallelic transcription increased over the course of a response, a finding that has implications for immune memory and autoimmunity. This technique may have broad applications in mouse models of human disease.

Introduction

Recent advances have allowed us to analyze the development and persistence of virus-specific CD8+ T cell–mediated immunity from naive CTL precursors (CTLps) in peripheral lymphoid tissue, through the antigen-driven phase in lymph nodes and spleen, to the CTL effectors in a site of virus-induced pathology, and then, ultimately, to the persistence and recall of immune memory (1–3). However, unless we use lymphocytes from TCR-transgenic mice, our capacity to follow the fate and persistence of defined clonotypes is very limited. Several approaches have been used to estimate the extent of TCR diversity and to track clonally expanded T cell populations throughout the course of antigen-specific CTL responses (4), but none has given the complete picture. A commonly used protocol is to double-stain CD8+ T cells with mAbs specific for TCR variable (V) region β (TRBV) and tetramers specific for peptide+ class I MHC glycoprotein (pMHCI) epitopes (5–9). Such low-resolution analysis provides no insight into the extent of clonal diversity within a particular TRBV-specific population and offers little scope for determining the spectrum of TCRα usage, as there are few mAb reagents. Another approach, known as immunoscope or spectratyping, uses gel electrophoresis of total mRNA from TRBV-specific populations (RT-PCR product) to determine profiles of complementarity-determining region 3β (CDR3β) length (4, 10). Combining spectratyping with cloning and sequencing allows for more definitive identification of CDR3β transcripts, but the approach is compromised by the possibility of bias during the process of amplification from the RNA pool (10).

Any such skewing effect can be totally avoided by using single-cell RT-PCR of flow cytometer–sorted, epitope-specific CD8+

CTLs to define the spectrum of CDR3β usage within a particular responding T cell population (9, 11–14). This approach has allowed us to determine the spectrum of TRBV recruitment for a range of influenza epitope–specific CD8+ CTL responses within dominant TRBV populations using TRBV-specific primers. A few studies have used primer panels to amplify TRAV, but were not extensively characterized to show total repertoire coverage (15, 16). However, in the absence of any contemporary single-cell analysis of TRAV as well as of an unbiased TRBV method, we have not been able to measure the true extent of clonal diversity for CD8+ CTL effector populations recovered directly from virus-infected individuals (10). The same is true for those analyzing the relative prevalence of T cell clones in diseases like HIV/AIDS (17, 18).

Here, we describe an extension of the single-cell RT-PCR protocol, a technique that allowed for simultaneous identification of CDR3α and CDR3β transcripts from the same responding T cell, without the necessity for any prior knowledge of specific TRAV or TRBV usage. This protocol has wide applications, allowing tracking of endogenous clonotypic responses, complete characterization of the responding paired α/β TCR repertoire, and investigation of TCRα chain regulation during immune activation.

Results

Amplification of CDR3α and CDR3β from single CD8+ T cells. Using a multiplex, nested PCR-based assay, we successfully amplified TCR CDR3α and CDR3β transcripts from epitope (KbPB1703) specific CD8+ T cells (19) isolated directly from the inflamed airways of influenza virus–infected mice (Figure 1, A and B). In general, the success rate of amplification with this method was approximately 45%–65% for CDR3α and 55%–75% for CDR3β. The purified KbPB1703+ TCRα and TCRβ CDR3 PCR products were then sequenced using internal constant chain (C; i.e., TRAC and TRBC) reverse primers, allowing
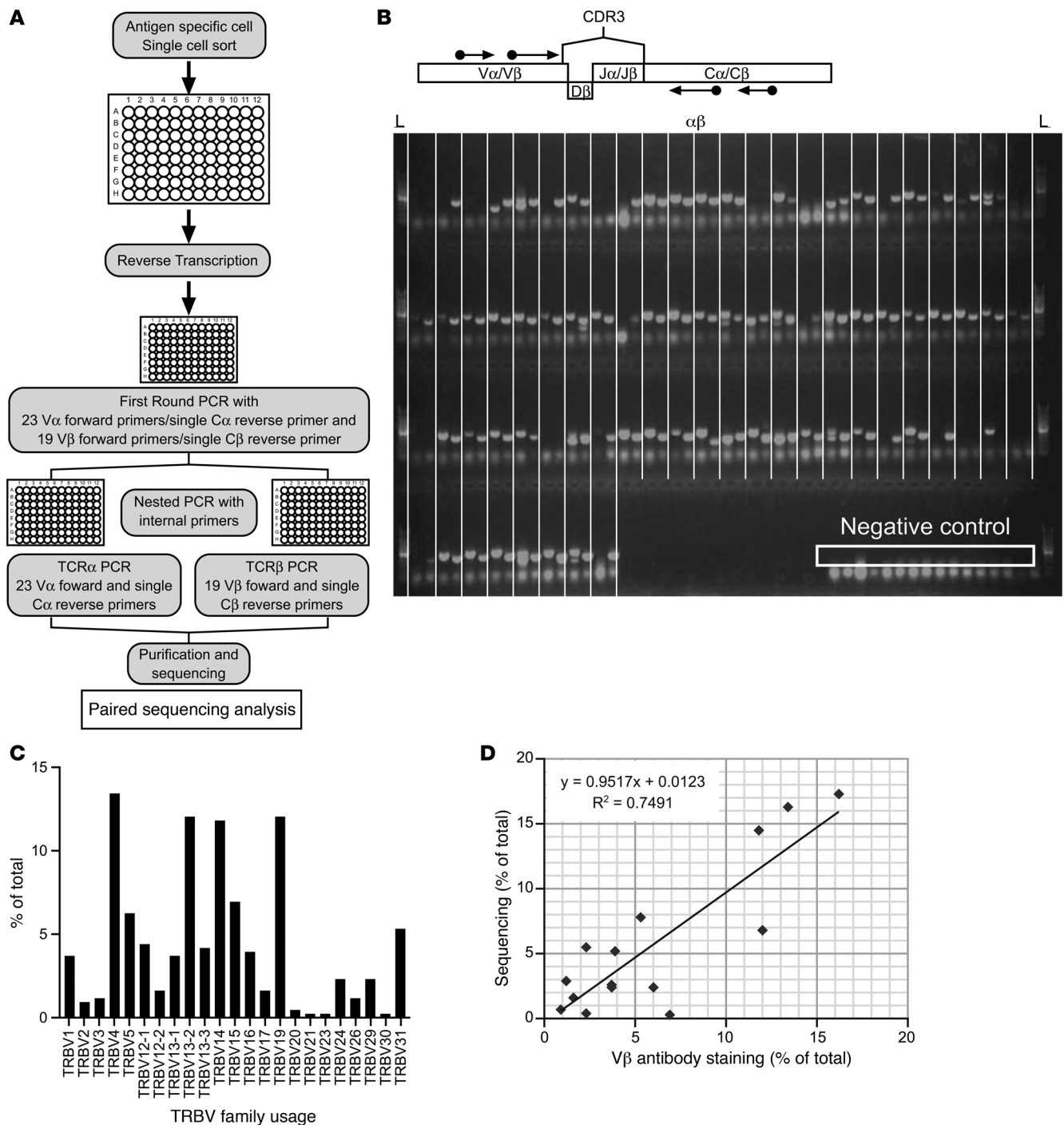
Figure 1
Unbiased single-cell amplification of TCR CDR3α and CDR3β. (**A**) Schematic diagram of the multiplex PCR method used to simultaneously amplify and sequence the TCR CDR3α and CDR3β regions. Following single-cell sorting of $K^bPB1_{703}^+CD8^+$ T cells into a PCR plate, the first round of PCR used a primer mixture of 23 TRAV and 19 TRBV forward and single TRAC and TRBC reverse primers. Subsequently, a nested PCR was performed for α and β in a separate plate using a corresponding internal primer mix (23 TRAV forward, single TRAC reverse, and 19 TRBV forward, single TRBC reverse, respectively). (**B**) Schematic representation of the TCR CDR3 region, showing the relative positions of the oligonucleotide primers. An agarose gel electrophoresis image of TCR segments containing CDR3α and CDR3β amplified from single $K^bPB1_{703}^+CD8^+$ T cells is also shown. L, 100-bp ladder lane. The α and β products were loaded alternately in each twin-lane (separated by vertical lines). Negative control PCR reactions (for contamination) without any cDNA are shown in the boxed region. (**C**) TRBV usage in the primary $K^bPB1_{703}^+CD8^+$ T cell response determined by multiplex RT-PCR and sequencing ($n = 9$ mice). (**D**) Correlation of the data in **C** to data acquired by costaining tetramer-specific $K^bPB1_{703}^+CD8^+$ T cells with a panel of anti-TRBV antibodies.
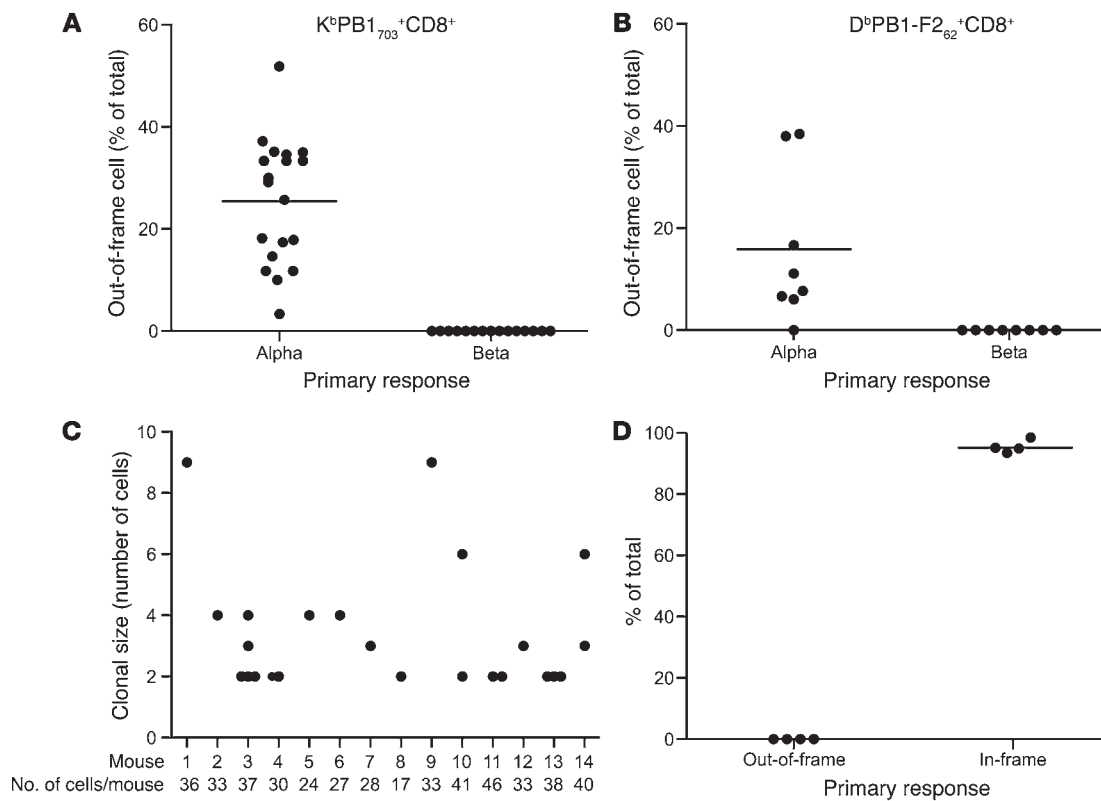
Figure 2
Prevalence of out-of-frame TCRα transcripts in influenza epitope–specific peripheral CD8+ T cells. Single-cell analysis of $K^bPB1_{703}^+CD8^+$ T cells (**A**) or $D^bPB1-F2_{62}^+CD8^+$ T cells (**B**) obtained by BAL (day 10) from infected mice showed that 25% (of the 650 cells analyzed from 19 mice) and 15.6% (of the 192 cells analyzed from 8 mice) of total cells, respectively, expressed an out-of-frame *Tcra* transcript, whereas all *Tcrb* transcripts were in-frame. Each dot represents a single mouse. (**C**) Clonal frequency (25 clones from 14 mice) of individual out-of-frame sequences, with each dot representing a single clone. We considered 2 or more cells with identical CDR3α/CDR3β pairing as clonal. The number of sequences analyzed per mouse is shown. (**D**) Analysis of $K^bPB1_{703}^+CD8^+$ T cells from the BAL of $Tcra^{-/+}$ mice on day 10 after primary infection showed no out-of-frame *Tcra* sequences. Each dot represents a single mouse.

us to pair the coexpressing CDR3α and CDR3β sequences from the same well (Supplemental Table 1; supplemental material available online with this article; doi:10.1172/JCI44752DS1). The fact that we only ever observed 1 CDR3β transcript per well leaves us in no doubt that we are looking at the spectrum of TCR mRNA expression from single, epitope-specific T cells. A representative dataset of TCRα and TCRβ coexpression on $K^bPB1_{703}^+CD8^+$ CTLs from BAL of a mouse infected with HK×31 influenza A virus (H3N2; referred to herein as ×31) for 10 days is shown in Supplemental Table 1. The TCRα and TCRβ sequences could also be assigned with respective TRAV/TRAJ and TRBV/TRBD/TRBJ families (see Supplemental Table 1) by using an in-house developed BLAST analysis software querying the International ImMunoGeneTics information system (IMGT) database (20). An important caveat is that in certain families of TRAV genes, the closeness of the TRAV internal primer to the CDR3 region results in ambiguous family assignment. As shown in Supplemental Table 1, 4% of the sequences had 2 different TRAV family assignments with more than 99% similarities. In this case, if absolute assignment is needed for receptor expression, performing seminested PCR with the external forward primer can give greater accuracy in calling family names.

Validation of multiplex single-cell TCRβ RT-PCR method. Having successfully amplified and sequenced the complementary CDR3α

and CDR3β transcripts from individual $K^bPB1_{703}^+$ CTLs, we then sought to confirm that the spectrum of TRBV usage determined by this approach is broadly in accordance with the profiles of TRBV protein expression determined by the established mAb staining protocol for tetramer+CD8+ T cells. In addition to the profile of prominent Vβ8.1/8.2 (TRBV13-3/13-2), Vβ10b (TRBV4), Vβ13 (TRBV14), and Vβ14 (TRBV31) usage observed by flow cytometric analysis using a TRBV-specific mAb panel, our CDR3β multiplex RT-PCR TCR transcriptome protocol also showed that Vβ6 (TRBV19) and Vβ1 (TRBV5) figured in this K^bPB1_{703}-specific response (Figure 1C), highlighting the greater acuity of this mRNA-based protocol (Supplemental Table 2). Overall, there was good correlation between the profiles of preferred TRBV usage derived from our single-cell multiplex RT-PCR method and the standard, flow cytometry TRBV mAb scan for the K^bPB1_{703}-specific response (Figure 1D). The relative lack of mAbs meant that a similar comparison was not possible for the TCRα chain.

Occurrence of peripheral influenza epitope–specific CD8+ T cells with a nonproductive Tcra mRNA. The in vivo analysis focused directly on $K^bPB1_{703}^+CD8^+$ CTL effectors recovered from the inflamed airways of naive mice that had been infected with the relatively avirulent ×31. Surprisingly, single-cell RT-PCR at the peak of the primary response on day 10 showed the presence of nonproductive or out-
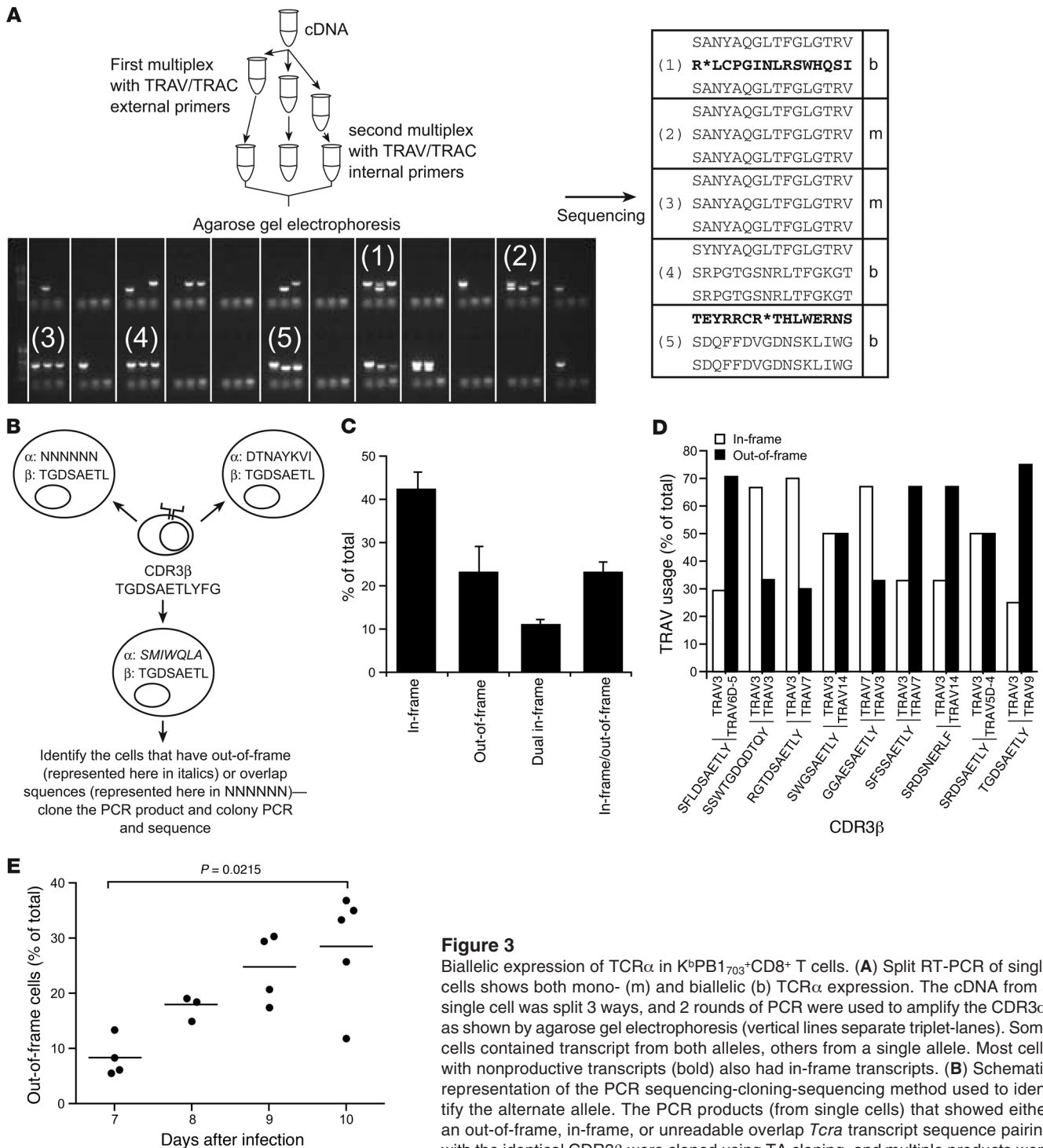
Figure 3
Biallelic expression of TCRα in K^bPB1_703^+CD8^+ T cells. (**A**) Split RT-PCR of single cells shows both mono- (m) and biallelic (b) TCRα expression. The cDNA from a single cell was split 3 ways, and 2 rounds of PCR were used to amplify the CDR3α, as shown by agarose gel electrophoresis (vertical lines separate triplet-lanes). Some cells contained transcript from both alleles, others from a single allele. Most cells with nonproductive transcripts (bold) also had in-frame transcripts. (**B**) Schematic representation of the PCR sequencing-cloning-sequencing method used to identify the alternate allele. The PCR products (from single cells) that showed either an out-of-frame, in-frame, or unreadable overlap *Tcra* transcript sequence pairing with the identical CDR3β were cloned using TA cloning, and multiple products were sequenced. (**C**) The percentage of cells that had 2 transcripts (dual–in-frame and in-frame/out-of-frame) was 35%. In addition, approximately 42% and 23% of all cells analyzed had a monoallelic productive or nonproductive transcript, respectively (data derived from 3 mice and 240 split reactions). Values are mean ± SEM. (**D**) Comparing nonbiased amplification of TCRα by TRAV primers. Relative frequencies of in-frame and out-of-frame TCRαs paired with the same TCRβ showed that the varying efficiency of amplification was clone specific, rather than TRAV specific (data derived from 78 sequences from 5 mice). (**E**) K^bPB1_703^+CD8^+ T cells were analyzed on days 7, 8, 9, and 10 after primary virus challenge (672 cells from 16 individual mice) for the proportion of the total response represented by out-of-frame cells, showing a significant change ($P = 0.0215$) between day 7 and day 10.

Table 1
Identification of the other allele in single $K^bPB1_{703}^+CD8^+$ T cells

Cell	Original sequence data		Cloning and sequencing data		
	α	β	α	α (second allele)	β
A6	Overlap	SLDSAETLYFG	*STGVITRGSLSLDREP*	SENYAQGLTFGLGTRV	SLDSAETLYFG
A7	Overlap	TGTSAETLYFG	**SANYAQGLTFGLGTRV**	**SYNTNTGKLTFGDGTV**	TGTSAETLYFG
A4	*SMIWQLATHLWIWNPT*	TGDSAETLYFG	DTNAYKVIFGKGTHLH	*SMIWQLATHLWIWNPT*	TGDSAETLYFG
B6	*SMIWQLATHLWIWNPT*	TGDSAETLYFG	DTNAYKVIFGKGTHLH	*SMIWQLATHLWIWNPT*	TGDSAETLYFG
C2	*SMIWQLATHLWIWNPT*	TGDSAETLYFG	DTNAYKVIFGKGTHLH	*SMIWQLATHLWIWNPT*	TGDSAETLYFG
F1	*SPQLPVWGNCSLEQE*	SSSSAETLYFG	*SPQLPVWGNCSLEQEP*	SGNYAQGLTFGLGTRV	SSSSAETLYFG
F2	Overlap	TGSSAETLYFG	**SNSNNRIFFGDGTQLV**	**SANYAQGLTFGLGTRV**	TGSSAETLYFG

Out-of-frame CDR3α clonotypes are italicized; dual–in-frame alleles are shown in bold.

of-frame *Tcra* transcripts in a number of the $K^bPB1_{703}^+CD8^+$ T cells. Extending this analysis to 650 TCRα sequences from 19 infected mice, the frequency of nonproductive mRNAs in multiple experiments was found to vary from 3% to 52%, with an average of 25% (Figure 2A). Concerned that these transcripts were the sole CDR3α product recovered, we also looked at a second epitope-specific CTL population, the $D^bPB1\text{-}F2_{62}$ set, with comparable results (Figure 2B). Furthermore, the occurrences of the out-of-frame *Tcra* transcript–bearing cells in the peak of the primary response appeared to be clonal (Figure 2C). On the other hand, none of the 540 CDR3βs analyzed by this multiplex method for $K^bPB1_{703}^+CD8^+$ or $D^bPB1\text{-}F2_{62}^+CD8^+$ T cells had nonproductive rearrangements (Figure 2, A and B), consistent with other CDR3β profiles analyzed by our research group over a number of years (9, 12–14).

To rule out that the nonproductive transcripts detected in these single cells reflected some PCR amplification artifact, we repeated the single-cell analysis of CDR3α transcripts for $K^bPB1_{703}^+CD8^+$ T cells from influenza virus–infected $Tcra^{-/+}$ hemizygous mice. Although these $Tcra^{-/+}$ hemizygotes can only generate productively rearranged TCRα chains from 1 chromosome, they are phenotypically and functionally normal (21, 22). As shown in Figure 2D, our conclusion that conventional $Tcra^{+/+}$ mice indeed express nonproductive transcripts from 1 of the 2 available TCRαs was confirmed by the observation that no such transcripts were detected in 237 sequences from 4 influenza virus–infected $Tcra^{-/+}$ mice.

Evidence of allelic modulation in influenza-specific peripheral CD8+ T cells. Since all the epitope-specific cells were isolated by K^bPB1_{703} tetramer binding, we assumed that those lymphocytes with nonproductive *Tcra* transcripts must also express a productive TCRα chain in order to form a functional TCRαβ heterodimer. We used 2 approaches to identify the productive *Tcra* transcript in out-of-frame cells. The first was a split PCR protocol (23), in which the input cDNA, reverse transcribed from individual cells, was split among 3 wells and amplified separately (Figure 3A). The second protocol depended on cloning and sequencing the original nested PCR product that had a nonproductive transcript (Figure 3B). Using these methods, we were able to capture the expression of 2 *Tcra* transcripts from single cells expressing a nonproductive transcript, with the second chain representing an in-frame rearrangement. Additionally, T cells that expressed 2 in-frame transcripts (Figure 3C) were found to account for approximately 10% of the tetramer+CD8+ population. These dual–in-frame CTLs have the potential to recognize 2 distinct and non–cross-reactive pMHCI epitopes, making them of considerable interest in light of the much-discussed possibility that virus infections may trigger auto-

immunity (24, 25). The percentage of cells that had 2 transcripts (both dual–in-frame and in-frame/out-of-frame), as measured by the split PCR method, was 35%, derived from examination of 3 mice and 240 split reactions (Figure 3C). In addition, a mean of 42% and 23% of total cells were found to express a productive or a nonproductive transcript, respectively (Figure 3C). Again, as these cells were sorted for tetramer binding specificity, we assumed that this latter group must contain an as-yet undetected in-frame rearrangement, making the total percentage of TCRα biallelic cells approximately 60% at this time point (day 10 after infection). Furthermore, when looking within the same individual, we found other cells containing the same productive CDR3α/CDR3β rearrangements, also paired with the same nonproductive CDR3α (Table 1 and data not shown), which indicates that these are the progeny of clonally expanded CTLps. This phenomenon — cells with a particular CDR3β chain but different CDR3α chains representing a clonal population — was found in a different context by Hamrouni et al. (16).

Could the selective amplification of individual TCRα chains in our protocol result from efficiency differences among the TRAV primer families that give the appearance of modulation at the transcript level? Using the data across different mice in which a nonproductive and productive *Tcra* transcript was associated with a single CDR3β, we tested for a preferential PCR efficiency effect by analyzing the frequency of specific TRAV regions for nonproductive and productive transcripts from these clonotypes. That is, we sought to determine whether particular TRAV regions are consistently amplified over others in cases where transcripts for 2 CDR3αs are found in the same CTLp. The data in Figure 3D (78 T cells from 5 different mice) shows a frequency analysis for situations in which 2 TRAV products were paired with 1 specific CDR3β. The varying frequencies of amplification of these TRAV families across the population indicated that this phenomenon is not some reflection of preferential PCR efficiency for particular TRAV primers. For example, in the clonal cell population where RGTDSAETLY was the CDR3β, the in-frame TRAV3 dominated, while the out-of-frame TRAV7 product was detected at a lower frequency. Conversely, in the clonal population with the GGAE-SAETLY CDR3β sequence, the exact same 2 TRAV regions were found, but their detection frequency was inverted (Figure 3D). If PCR bias were contributing to this result, we would expect to find the preferred allele consistently; instead, the allelic dominance was cell specific rather than sequence specific (Figure 3D).

Antigen-specific CD8+ T cells with nonproductive TCRα increase over the course of an inflammatory response. The repeated observation of

clonal populations in which only one allele was detected by the initial RT-PCR analysis and the split PCR protocol, but both alleles were clearly being expressed, provides strong evidence for transcriptional modulation of allele expression. One hypothesis suggested by this finding is that allelic modulation varies over the course of an inflammatory response. To test this, we used the relative level of out-of-frame cells as a proxy for allelic modulation — as the data in Figure 3, A and B, and Table 1 demonstrated that all out-of-frame cells were by definition dual mRNA expressers. We sorted $K^bPB1_{703}^+CD8^+$ T cells on days 7, 8, 9, and 10 after infection and determined the percentage of cells expressing an out-of-frame cell $TCR\alpha$ allele. Intriguingly, the frequency of out-of-frame cells increased significantly ($P = 0.0215$) between days 7 and 10 after infection, as measured for a total of 672 sequences from 16 mice (Figure 3E). The upregulation of the dual $TCR\alpha$ phenotype may have important functional implications for these peripheral effector cells, including generating novel, nonselected specificities under inflammatory conditions or, in the case of nonfunctional gene expression, reducing TCR signaling potential by limiting functional TCR expression.

Discussion

We report the development of a technique, which we believe to be novel, for amplifying and direct sequencing $TCR\alpha$ and $TCR\beta$ chains directly ex vivo from a single cell. The $TCR\beta$ repertoire has proved to be an important functional determinant of T cell quality in a number of model systems (10). Additionally, although multiple clonotypic lineages might contain the same $TCR\beta$, the combination of dual $TCR\alpha$ chains paired with a specific $TCR\beta$ chain provides a more unique $CDR3\alpha/\beta$ signature for tracking. This will allow endogenous studies similar to the recently reported barcoding technique, but without the necessity of viral transduction and adoptive transfer (26, 27). Of course, we cannot distinguish between cells derived from a single, peripheral naive progenitor and cells that had undergone homeostatic expansion. Furthermore, although deep sequencing technology has expanded the scope to which α or β CDR3 regions can be sequenced in bulk (28), only a single-cell–based analysis can measure the true repertoire diversity. Given the difficulties previously encountered with analysis of the $CDR3\alpha$ resulting from its broad diversity, this approach represents the first ex vivo analysis to our knowledge of $TCR\alpha$ expression during an antigen-specific response.

The usefulness of this study in generating large numbers of distinct antigen-specific T cell receptors is immediately apparent, as similar technology is now used for specific Ig expression (29). However, the existence of dual–in-frame cells may result in the wrong in-frame $TCR\alpha$ chain being chosen for expression. Still, our results suggest that this phenomenon is present in approximately 10% of antigen-specific cells. Similarly, to obtain the antigen-specific receptor, an out-of-frame result would need to be followed by cloning to obtain the in-frame allele, which we were able to obtain in 100% of tetramer+ cells. The high prevalence of CTLs with nonproductive *Tcra* transcripts (Figure 2, A and B) was surprising. It is possible that stochastic PCR competition could result in observation of out-of-frame cells without representing transcriptional dominance of the out-of-frame allele. However, we did not find any preferential bias for particular V regions across multiple pairs of coexpressed $TCR\alpha$ alleles, in which the out-of-frame transcript was dominant over the in-frame transcript (Figure 3B). Further, in our split PCR method of determining the repertoire in single cells (Figure 3A), we found cells

with a particular in-frame $CDR3\alpha$ (e.g., SANYAQGLTFGLGTRV) in all the split reactions from a single cell, whereas in some cells derived from the same clonal precursor, we found an out-of-frame $CDR3\alpha$ transcript in addition to the expected in-frame $CDR3\alpha$ (e.g., SANYAQGLTFGLGTRV and R*LCPGINLRSWHQSI) in different split reactions. This observation suggests that the detection of any particular TRAV (representing either an out-of-frame or an in-frame transcript) reflects the amount of transcript present and not the result of primer competition.

Allelic exclusion is known to be a relatively inefficient process for $TCR\alpha$ (30–32). In some circumstances, phenotypic exclusion has been reported to efficiently downregulate the nonselected, nonspecific product at the protein level. In Ig and $TCR\beta$ chain, a process known as nonsense-mediated mRNA decay (NMD) has been suggested as a control mechanism for limiting the transcription and subsequent translation of these prematurely terminated mRNAs (33–37). Similar mechanisms could also play a role in downmodulating nonproductively rearranged *Tcra* mRNAs. Indeed, although detection of nonproductive transcripts in $CDR3\alpha$ and $CDR3\beta$ PCR products from total mRNA of antigen-specific clones has been described previously (31), we failed to detect any nonproductive *Tcrb* transcript in our single-cell analysis. The detection frequency of nonproductive *Tcra* transcript only has been previously reported to be very low in a single-cell analysis of immunized mice, although it is possible that the low frequency of $CDR3\alpha$ transcripts reported may be due to the limited set of TRAV primers used in that study (16). In contrast, we recovered multiple $CD8^+$ T cells bearing the same nonproductive *Tcra* mRNA paired with 1 *Tcrb* from the infected lungs of 14 of 19 mice (data not shown), indicating that these tetramer+$CD8^+$ CTLs are functioning somewhat normally, at least with respect to clonal expansion in lymphoid tissue and trafficking to a site of inflammatory pathology.

The increase in the prevalence of out-of-frame cells during the course of the primary response was very interesting. This may be a result of conversion from the in-frame antigen-specific cells that were recruited to the immune response to an out-of-frame phenotype by allelic modulation. However, it is also possible that cells with the out-of-frame phenotype are differentially recruited, appearing later in the response. Ongoing experiments are addressing this possibility; however, we found that the degree of tetramer binding did not correlate with out-of-frame expression (our unpublished observations).

In summary, we describe a technique that allows the simultaneous amplification of $TCR\alpha$ and $TCR\beta$ chain transcripts from single T lymphocytes recovered directly ex vivo. This protocol, which allows us to track T cell clonotypes throughout an infection, showed a startling level of dual-allele expression for $TCR\alpha$ (but not $TCR\beta$) chains, with dual–in-frame and in-frame/out-of-frame mRNA combinations accounting for approximately 60% of the CTLs recovered from the lungs of mice with influenza pneumonia. Additionally, the fact that T cells with the potential to express 2 functional $TCR\alpha$ chains (dual–in-frame) had passed through thymic selection raises the possibility that clonotypes bearing TCRs that have not been subject to effective negative selection may translate to the periphery, where expression of the second allele is markedly enhanced in response to an inflammatory response. Furthermore, the fact that the incidence of 2-TCR CTLs expands during a virus infection, and that these cells locate to distal, nonlymphoid tissue sites, has implications for the induction of autoimmunity (25, 38–40). This possibility is now under active investigation in

our laboratory, as is the further analysis of our finding that these T cells with dual *Tcra* transcripts did not contribute to long-term memory. If that is indeed the case, the risk of triggering autoimmunity as a consequence of infection may be reduced.

Methods

Mice, infection, and reagents. Female C57BL6/J mice were obtained from The Jackson Laboratory at 4–6 weeks of age and maintained in the Animal Resource Center at St. Jude Children's Research Hospital under an IACUC-approved protocol. The TCR hemizygous ($Tcra^{-/+}$) mice were generated by crossing the C57BL6/J and B6.129S2-$Tcra^{tm1Mom}$/J ($Tcra^{-/-}$) strains. Naive (primary) mice were infected intranasally with 10^6 egg ID_{50} of ×31. Inflammatory cells were recovered from the lung by bronchoalveolar lavage (BAL) on day 10 after primary infection. Antigen-specific CD8+ T cells were stained with fluorochrome-conjugated tetrameric complexes of the H2K^b MHC class I glycoprotein and the influenza PB1$_{703–711}$ (SSYRRPVGI) peptide or H2D^b plus the PB1-F2$_{62–71}$ (LSLRNPILVF) peptide (obtained from Trudeau Institute). All antibodies were purchased from BD Biosciences — Pharmingen unless otherwise indicated.

Single-cell sorting. After removing the erythrocytes using rbc lysis buffer (8.3 g NH$_4$Cl, 1 g KHCO$_3$, and 1 ml 0.1% Phenol Red in 1 l distilled water), the BAL cells were treated with Fc block (rat anti-mouse CD16/CD32) and then stained using allophycocyanin- or PE-conjugated K^{b}PB1$_{703}$ tetramer at room temperature for 1 hour, followed by eFluor780- or allophycocyanin-conjugated anti-CD8 antibody (clone 53-6.7, eBiosciences), FITC-conjugated anti-CD4, anti-mouse pan-macrophage marker BM8 (F4/80), anti-mouse CD11c, and anti-mouse CD11b for 20 minutes on ice. The non-CD8+ T cells were excluded using a dump gate based on CD4, F4/80, CD11c, and CD11b staining. In some experiments, the K^{b}PB1$_{703}$+CD8+ T cells were also stained using a panel of TRBV-specific antibodies (12, 13). The tetramer+CD8+ T cells were suspended in buffer (PBS containing 2% BSA and 200 U RNAsin/ml, Promega) and deposited as single cells into the wells of a 96-well PCR plate (Biorad) using a MoFlo flow cytometer (Cytomation) fitted with a Cyclone single-cell deposition unit. The last 2 columns of the plate were left blank for negative controls. After sorting, the plates were sealed using adhesive films and frozen at –80°C prior to RT-PCR. The staining profile and gating strategy is shown in Supplemental Figure 1.

Design of oligonucleotide primers for CDR3α and CDR3β amplification. A nested, single-cell, multiplex PCR approach was used to amplify the CDR3α and CDR3β TCR regions from individual T cells. Known functional and open reading frame nucleotide sequences of the TCRα and TCRβ families were retrieved from the IMGT database (http://www.imgt.org; ref. 20). For the TCRα chain, there were 82 different functional and open reading frame TRAV sequences. These sequences were grouped in a phylogenetic tree, and the forward oligonucleotide primers (both external and internal) were designed (Supplemental Table 3) to amplify closely related TRAV sequences. When a consensus region could not be found, degenerate bases were used in the primer design to amplify these groups. In contrast, the TRBV families were substantially less diverse. Therefore, the TRBV-specific forward oligonucleotide primers (both external and internal) were designed to amplify individual V regions, except in the case of multisequence families like TRBV12 and TRBV13 where a single oligonucleotide was designed to amplify all family members (Supplemental Table 4). In total there were 23 TRAV and 19 TRBV forward primers each for external and internal rounds of PCR. The antisense oligonucleotides primers (both external and internal) for TCRα and TCRβ were designed from TRAC and TRBC sequences, respectively. All oligonucleotide primers were synthesized at the Hartwell Centre of St. Jude Children's Research Hospital and validated using cDNA as template from total RNA isolated from resting CD8+ T cells (Supplemental Figure 2). The positions of the primers are shown in Figure 1B.

Single-cell RT-PCR, sequencing, and cloning. cDNA synthesis was performed directly from single cells using the iScript cDNA Synthesis Kit (Bio-Rad) per the manufacturer's instructions, with minor modifications. The cDNA synthesis used 2.5 μl of reaction mix consisting of 0.5 μl 5× iScript reaction mix, 0.5 μl iScript reverse transcriptase, and 0.1% Triton X-100 (Sigma-Aldrich), with the remainder H$_2$O. This was incubated at 25°C for 5 minutes, 42°C for 30 minutes, and 85°C for 5 minutes. Following RT, a multiplex nested PCR was done with a Taq polymerase–based PCR kit (Qiagen) to amplify the CDR3α and CDR3β transcripts from each cell in a 25-μl reaction mix containing 2.5 μl cDNA. The first round of PCR was performed with 2.5 μl of 10× PCR buffer containing 15 mM MgCl$_2$, 0.5 μl 10 mM dNTP, 0.75 U Taq DNA polymerase, and 0.5 μl oligonucleotide mixture of 23 TRAV forward and single TRAC reverse along with 19 TRBV forward and single TRBC reverse oligonucleotides (each 5 μM final concentration; Supplemental Tables 3 and 4). When cells were sorted with a particular TRBV antibody, the primers (both sense and antisense, 5 μM each) used were specific for that family. A second round of nested PCR was then performed for CDR3α and CDR3β using product from the first PCR round as template and a similar primer mixture for the TRAV and TRBV internal primers. For the split PCR protocol, the cDNA from a single cell was diluted to 10 μl using water and then divided into 3 wells. The first- and second-round PCR was then done as described above. The PCR conditions were 95°C for 5 minutes followed by 34 cycles of 95°C for 20 seconds, 56°C for 20 seconds, and 72°C for 45 seconds, with a final extension at 72°C for 7 minutes. A schematic of the PCR strategy is shown in Figure 1A. The PCR products were visualized on a 2% agarose gel, then purified using a Wizard SV40 PCR purification kit (Promega) and sequenced using TRAC or TRBC reverse primers for α and β PCR products, respectively, using a ABI Big Dye sequencer (Applied Biosystem) at the Hartwell Centre of St. Jude Children's Research Hospital.

For the PCR cloning studies (see Figure 3B), cells with nonproductive transcripts were identified from the sequence analysis by their well number. The corresponding, purified PCR products were then cloned into a TOPO TA cloning vector (Invitrogen). Individual clones were picked, and colony PCR was performed using M13 forward and reverse primers. The PCR products were then purified as before and sequenced using TRAC reverse primers.

TRBV antibody scan. Cells isolated from the BAL of infected mice were stained with allophycocyanin- or PE-conjugated K^{b}PB1$_{703}$ tetramer, eFluor780- or allophycocyanin- conjugated anti-CD8 antibody (clone 53-6.7, eBiosciences), and a panel of FITC-conjugated anti-TRBV antibodies (Vβ2, clone B20.6; Vβ3, clone KJ25; Vβ4, clone KT4; Vβ5.1/5.2, clone MR9-4; Vβ6, clone RR4-7; Vβ7, clone TR310; Vβ8.1/8.2, clone MR5-2; Vβ8.3, clone 1B3.3; Vβ9, clone MR10-2; Vβ10b, clone B21.5; Vβ11, clone RR3-15; Vβ12, clone MR11-1; Vβ13, clone 12-3; Vβ14, clone 14-2; Vβ17a, clone KJ23; all from BD Biosciences — Pharmingen). The TRBV usage frequencies were then determined by flow cytometry.

Data analysis. The sequence data for CDR3α and CDR3β were analyzed using Chromas (Technelysium Pty Ltd.) and MegAlign Software (DNASTAR Lasergene) and processed using an Excel spreadsheet containing macros (from http://www.bioc.uzh.ch/antibody) that parse the nucleotide sequences and convert them to amino acid sequences (41). The results were tabulated in the same spreadsheet for paired coexpression analysis. The TRAV/TRAJ and TRBV/TRBD/TRBJ assignments were obtained using an in-house Web application written in PHP 5 and MySQL 5. The TCR Web application allows users to upload FASTA files individually or in zipped archives and queries them against the IMGT T-Cell Receptor online database using PHP cUrl. The HTML returned from the IMGT Web site query is parsed using regular expressions to locate key features in the text. A table is printed at the top of the IMGT HTML results that allows the quick recognition of the overall results of the user query, such as whether the query succeeded, which receptor family names were found, and an amino acid translation of the receptor.

More specific information, such as the nucleotide sequence of the translation, is found further down in Results.

Several checks were in place in order to prevent erroneous reporting of null sequence results (false negatives). Additionally, we found that uploading sequences bounded by many unknown nucleotides (Ns) frequently generated false negatives or incorrect receptor family names. To avoid this, the TCR database truncated the number of Ns on either side of an uploaded sequence to 5, 6, or 7 Ns in such a way as to preserve the reading frame. False positives were easily prevented by the fact that IMGT does not display the receptor names if none are found, and the sections that contain the results of true positives are not displayed for genuine null sequences.

Statistics. Nonparametric Kruskal-Wallis ANOVA was used with Dunn posttest to determine individual significance (Figure 3E). All calculations were done using GraphPad software. A P value less than 0.05 was considered significant.

1. Obar JJ, Khanna KM, Lefrançois L. Endogenous naive CD8+ T cell precursor frequency regulates primary and memory responses to infection. *Immunity*. 2008;28(6):859–869.
2. Moon JJ, et al. Naive CD4+ T cell frequency varies for different epitopes and predicts repertoire diversity and response magnitude. *Immunity*. 2007; 27(2):203–213.
3. La Gruta NL, et al. Primary CTL response magnitude in mice is determined by the extent of naive T cell recruitment and subsequent clonal expansion. *J Clin Invest*. 2010;120(6):1885–1894.
4. Rufer N. Molecular tracking of antigen-specific T-cell clones during immune responses. *Curr Opin Immunol*. 2005;17(4):441–447.
5. Blattman JN, Sourdive DJ, Murali-Krishna K, Ahmed R, Altman JD. Evolution of the T cell repertoire during primary, memory, and recall responses to viral infection. *J Immunol*. 2000;165(11):6081–6090.
6. Busch DH, Pilip I, Pamer EG. Evolution of a complex T cell receptor repertoire during primary and recall bacterial infection. *J Exp Med*. 1998;188(1):61–70.
7. Valmori D, et al. Tetramer-guided analysis of TCR beta-chain usage reveals a large repertoire of melan-A-specific CD8+ T cells in melanoma patients. *J Immunol*. 2000;165(1):533–538.
8. Zhong W, Reinherz EL. In vivo selection of a TCR Vbeta repertoire directed against an immunodominant influenza virus CTL epitope. *Int Immunol*. 2004; 16(11):1549–1559.
9. Kedzierska K, Turner SJ, Doherty PC. Conserved T cell receptor usage in primary and recall responses to an immunodominant influenza virus nucleoprotein epitope. *Proc Natl Acad Sci U S A*. 2004; 101(14):4942–4947.
10. Turner SJ, Kedzierska K, La Gruta NL, Webby R, Doherty PC. Characterization of CD8+ T cell repertoire diversity and persistence in the influenza A virus model of localized, transient infection. *Semin Immunol*. 2004;16(3):179–184.
11. Maryanski JL, Jongeneel CV, Bucher P, Casanova JL, Walker PR. Single-cell PCR analysis of TCR repertoires selected by antigen in vivo: a high magnitude CD8 response is comprised of very few clones. *Immunity*. 1996;4(1):47–55.
12. Kedzierska K, et al. Terminal deoxynucleotidyltransferase is required for the establishment of private virus-specific CD8+ TCR repertoires and facilitates optimal CTL responses. *J Immunol*. 2008; 181(4):2556–2562.
13. La Gruta NL, et al. Epitope-specific TCRbeta repertoire diversity imparts no functional advantage on the CD8+ T cell response to cognate viral peptides. *Proc Natl Acad Sci U S A*. 2008;105(6):2034–2039.

14. Turner SJ, Diaz G, Cross R, Doherty PC. Analysis of clonotype distribution and persistence for an influenza virus-specific CD8+ T cell response. *Immunity*. 2003;18(4):549–559.
15. Baker FJ, Lee M, Chien Y-h, Davis MM. Restricted islet-cell reactive T cell repertoire of early pancreatic islet infiltrates in NOD mice. *Proc Natl Acad Sci U S A*. 2002;99(14):9374–9379.
16. Hamrouni A, Aublin A, Guillaume P, Maryanski JL. T cell receptor gene rearrangement lineage analysis reveals clues for the origin of highly restricted antigen-specific repertoires. *J Exp Med*. 2003; 197(5):601–614.
17. Douek DC, et al. A novel approach to the analysis of specificity, clonality, and frequency of HIV-specific T cell responses reveals a potential mechanism for control of viral escape. *J Immunol*. 2002; 168(6):3099–3104.
18. Price DA, et al. Public clonotype usage identifies protective Gag-specific CD8+ T cell responses in SIV infection. *J Exp Med*. 2009;206(4):923–936.
19. Belz GT, Xie W, Doherty PC. Diversity of epitope and cytokine profiles for primary and secondary influenza a virus-specific CD8+ T cell responses. *J Immunol*. 2001;166(7):4627–4633.
20. Lefranc M-P, et al. IMGT(R), the international ImMunoGeneTics information system(R). *Nucl Acids Res*. 2009;37(Database issue):D1006–D1012.
21. Corthay A, Nandakumar KS, Holmdahl R. Evaluation of the percentage of peripheral T cells with two different T cell receptor alpha-chains and of their potential role in autoimmunity. *J Autoimmun*. 2001; 16(4):423–429.
22. Elliott JI, Altmann DM. Dual T cell receptor alpha chain T cells in autoimmunity. *J Exp Med*. 1995; 182(4):953–959.
23. Esumi S, Kaneko R, Kawamura Y, Yagi T. Split single-cell RT-PCR analysis of Purkinje cells. *Nat Protoc*. 2006;1(4):2143–2151.
24. von Herrath MG, Oldstone MB. Virus-induced autoimmune disease. *Curr Opin Immunol*. 1996; 8(6):878–885.
25. Miller SD, Katz-Levy Y, Neville KL, Vanderlugt CL, Michael JB, Iain LC. Virus-induced autoimmunity: Epitope spreading to myelin autoepitopes in theiler's virus infection of the central nervous system. In: Buchmeier MJ, Campbell IL. Vol. 56 *Advances in Virus Research*. Burlington, Massachusetts, USA: Elsevier Inc.; 2001:199–217.
26. Gerlach C, et al. One naive T cell, multiple fates in CD8+ T cell differentiation. *J Exp Med*. 2010; 207(6):1235–1246.
27. Schepers K, et al. Dissecting T cell lineage relationships by cellular barcoding. *J Exp Med*. 2008;

205(10):2309–2318.
28. Wang C, et al. High throughput sequencing reveals a complex pattern of dynamic interrelationships among human T cell subsets. *Proc Natl Acad Sci U S A*. 2010;107(4):1518–1523.
29. Wrammert J, et al. Rapid cloning of high-affinity human monoclonal antibodies against influenza virus. *Nature*. 2008;453(7195):667–671.
30. Borgulya P, Kishi H, Uematsu Y, von Boehmer H. Exclusion and inclusion of alpha and beta T cell receptor alleles. *Cell*. 1992;69(3):529–537.
31. Casanova JL, Romero P, Widmann C, Kourilsky P, Maryanski JL. T cell receptor genes in a series of class I major histocompatibility complex-restricted cytotoxic T lymphocyte clones specific for a Plasmodium berghei nonapeptide: implications for T cell allelic exclusion and antigen-specific repertoire. *J Exp Med*. 1991;174(6):1371–1383.
32. Malissen M, Trucy J, Jouvin-Marche E, Cazenave PA, Scollay R, Malissen B. Regulation of TCR alpha and beta gene allelic exclusion during T-cell development. *Immunol Today*. 1992;13(8):315–322.
33. Gudikote JP, Wilkinson MF. T-cell receptor sequences that elicit strong down-regulation of premature termination codon-bearing transcripts. *EMBO J*. 2002;21(1–2):125–134.
34. Buzina A, Shulman MJ. Infrequent translation of a nonsense codon is sufficient to decrease mRNA level. *Mol Biol Cell*. 1999;10(3):515–524.
35. Delpy L, Sirac C, Magnoux E, Duchez S, Cogné M. RNA surveillance down-regulates expression of nonfunctional kappa alleles and detects premature termination within the last kappa exon. *Proc Natl Acad Sci U S A*. 2004;101(19):7375–7380.
36. Chemin G, et al. Multiple RNA surveillance mechanisms cooperate to reduce the amount of nonfunctional Ig{kappa} transcripts. *J Immunol*. 2010; 184(9):5009–5017.
37. Wang J, Vock VM, Li S, Olivas OR, Wilkinson MF. A quality control pathway that down-regulates aberrant T-cell receptor (TCR) transcripts by a mechanism requiring UPF2 and translation. *J Biol Chem*. 2002;277(21):18489–18493.
38. Gurevich VS. Influenza, autoimmunity and atherogenesis. *Autoimmun Rev*. 2005;4(2):101–105.
39. Sfriso P, et al. Infections and autoimmunity: the multifaceted relationship. *J Leukoc Biol*. 2010; 87(3):385–395.
40. Molina V, Shoenfeld Y. Infection, vaccines and other environmental triggers of autoimmunity. *Autoimmunity*. 2005;38(3):235–245.
41. Ewert S, Huber T, Honegger A, Plückthun A. Biophysical properties of human antibody variable domains. *J Mol Biol*. 2003;325(3):531–553.